Focusing Patterns within Far and Near Field for a Novel 2D Sparse MIMO Array

Harun Cetinkaya [*1], Simon Kueppers [*], Reinhold Herschel [*], Nils Pohl [*]

[*] *Fraunhofer Institute for High Frequency Physics and Radar Techniques, Fraunhoferstr. 20, D-53343 Wachtberg, Germany*

[1] harun.cetinkaya@fhr.fraunhofer.de

***Abstract*— A novel sparse 2 dimensional (2D) multiple-input-multiple-output (MIMO) array topology is proposed for 3D imaging. The highly compact, novel array only consists of 2 transmitters and 8 receivers. The focusing capabilities of the array are investigated by simulation and measurement data. The results for the focusing capabilities show that the array has a favorable maximum sidelobe level within far and near field.**

I. Introduction

Due to the high focusing and penetration capabilities of electromagnetic waves at millimeter range, there is a great interest on radar imaging systems [1]-[3]. However, the fact that SAR based systems require high measurement time [3], and radar arrays tend to be large and hard to install [2]. Therefore, radar imaging technology has not been used for robotic applications so far. To change this situation one of the key innovations within the SmokeBot project (H2020-ICT, [4]) is digitally steerable 3D radar sensor are realized based on integrated millimeter wave technology at 120 GHz. The short wavelength allows extremely small factor. However, the high degree of integration restricts the degrees of freedom of the array design.

There are typically two choises for 2D arrays, namely, conventional arrays in which transmitter and receiver are spatially co-located and multiple-input-multiple-output (MIMO) arrays in which transmitter and receiver are spatially dislocated. The major problem in conventional arrays arises from that sparseness, resulting in grating lobes, is mostly inevitable to decrease design complexity. In order to solve this matter, MIMO arrays based on novel MIMO typologies [5]-[7] can be solutions. However, these arrays should have a decent number of transmitters and receivers to achieve 3D imaging with a low grating/side lobe level.

During a MIMO array design using a low number of transmitters and receivers, the main challenge is that grating lobes, caused by sparseness due to the element size, exist in the region of interest and the energy of grating lobes can not be spread into whole radiation field due to the low number of elements.

This paper proposes a novel MIMO array topology which comprises 2 transmitters and 8 receivers, located at specific locations on the extremely compact array plane. The topology does not suffer from the design complexity and sparseness.

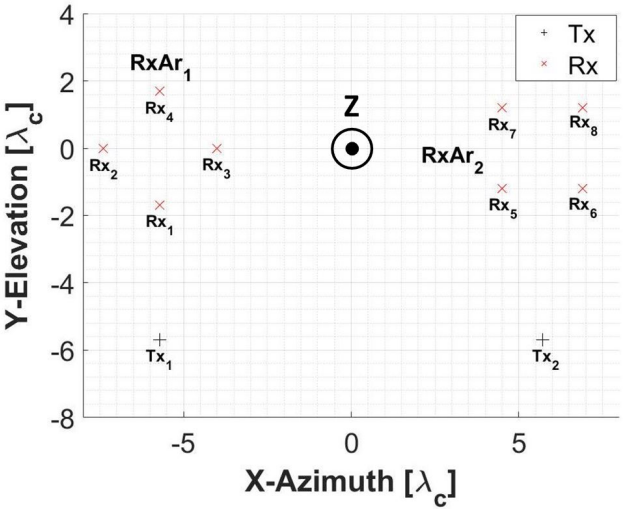

Fig. 1: 2D proposed MIMO array

The paper is organized as follows. Section II presents the geometry for the array in detail. In section III, the simulation and measurement methods are explained in brief and analyzes its focusing patterns within far and near field. Section IV investigates the imaging performance of the proposed array. Finally, section V summarizes the results and concludes this paper.

II. Array Description

As seen in Fig. 1, the proposed MIMO array topology has 2 transmitters and 8 receivers. The array element coordinates corresponding to the topology of Fig. 1, are normalized to the wavelength at the center frequency.

Two transmitters, labeled as Tx1 and Tx2 are located below two receive arrays, namely, RxAr-1 and RxAr-2. RxAr-1 and RxAr-2 are square arrays and each one consists of 4 receive elements but one turned by 45^o.

For the ease of the MIMO array design, especially, at millimeter-wave range, the receive element spacing in both receiver arrays is $2.401\ \lambda_c$ at the least. The distance between the center of two receiver arrays is $11.402\ \lambda_c$ which is identical to a distance between Tx1 and Tx2. It is clear that the array elements are sparsely located. This significantly reduces the

TABLE 1
ARRAY ELEMENTS' COORDINATE POSITIONS

Antenna element	Azimuth coordinate [λ_c]	Elevation coordinate [λ_c]
Tr1	-5.7	-5.7
Tr2	5.7	-5.7
Rc1	-5.701	-1.698
Rc2	-7.399	0
Rc3	-4.003	0
Rc4	-5.701	1.698
Rc5	4.5	-1.201
Rc6	6.902	-1.201
Rc7	4.5	1.201
Rc8	6.902	1.201

hardware effort required for routing the transmission lines to all antenna elements. One can see the coordinate of the MIMO array elements on Table 1.

As seen in Fig. 2, the virtual array of the MIMO array topology includes three virtual sub-arrays. VirtAr-1 and VirtAr-3 are the convolution of Tx1, RxAr-1 and Tx2, RxAr-2, respectively. VirtArr-2 is the convolution of Tx1, RxAr-2 and Tx2, RxAr-1. The focusing properties of the proposed MIMO array, obtained in this study, are for VirtAr-2. This means that during the digital beam forming, signals, simulated for transmit-receive pairs which create VirtAr-2 are considered. Because VirtAr-2 is identical to a circular array whose focusing pattern is the Bessel function of the first kind of zero order [8] or, in other words, the difference between the main lobe and the maximum sidelobe level (MSLL) is about 8 dB.

III. FOCUSING PATTER ANALYSIS

The point spread function (PSF) shows the image created by a single scatterer providing information about the focusing characteristics of arrays such as grating lobes, side lobes and main lobe. In simulations, the PSF is determined in the following way. Because for the proposed array far-field conditions start to be satisfied at distances longer than 1 m from the radar module [9], and the region of interest in [4] begins from 1 m to 10 m, a point-like scatterer is located in front of the array in a certain distance as the focal point (x = 0m; y = 1m; z = 0m) for the far field simulation and (x = 0m; y = 1m; z = 0m), (x = -0.2m; y = 1m; z = 0m) as the center and edge focal point for the near field simulation. The scattered signal is then calculated in frequency domain at 117 GHz center frequency with 12 GHz bandwidth. The data obtained is focused by using modified Kirchhoff migration algorithm (MKMA) and the 3D PSF is generated over both, cross-range and range. In order to present far field focusing pattern, the obtained image is angularly interpolated between $\theta(-40^o, 40^o)$ for $\phi = 0^o$ and $\phi = 90^o$ due to angular electromagnetic-wave interference existing. Here θ, ϕ represent polar angle and azimuthal angle, respectively. For near field focusing pattern presentation, the maximum value along its range dimension is selected.

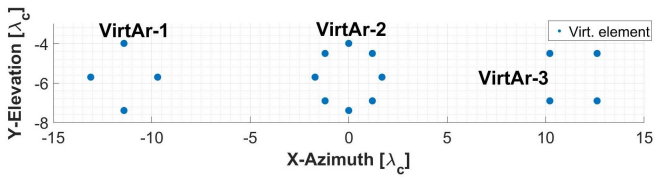

Fig. 2: Its virtual array

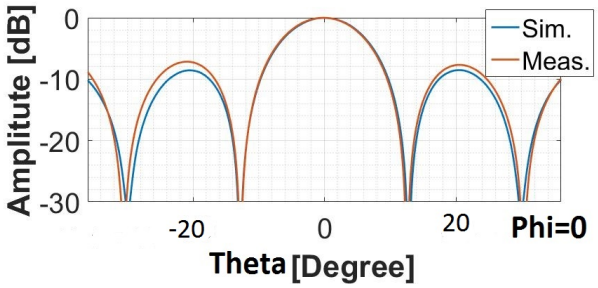

Fig. 3: Focusing pattern obtained along $\theta(-40^o, 40^o)$ for $\phi = 0^o$

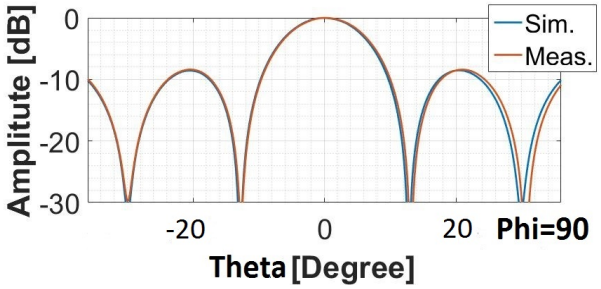

Fig. 4: Focusing pattern obtained along $\theta(-40^o, 40^o)$ for $\phi = 90^o$

For the measurement of focusing patterns, a small corner reflector whose size is about 1 cm for the length of the each edge is employed. It is located is at about 1 m from the center of the MIMO array and two measurements are performed. The former is for the focusing pattern calculation and the latter is for the calibration. Then, the measured data is calculated by using MKMA and its 3D PSF is generated. Far and near field measurement focusing patterns are then obtained with same methods mentioned above.

A. Far Field Focusing Pattern

In Fig. 3 and 4, the far field focusing patterns obtained by simulation and measurement are shown for the MIMO array. 3 dB beamwidth is defined by its virtual array aperture. As seen in Fig. 2, the virtual array considered is VirtAr-2. Because virtual elements within VirtAr-2 are distributed in a circle, the 3 dB beamwidth is symmetrical on each projection angle as seen in Fig. 3 and 4. Its main lobe is as narrow as 8.3^o in far field. The beamwidth obtained by simulation and measurement is consistent with the expected resolution, 1.5 m at 10 m range distance.

A circular array is generally supposed to have grating/sidelobe distributions in annular forms because of cir-

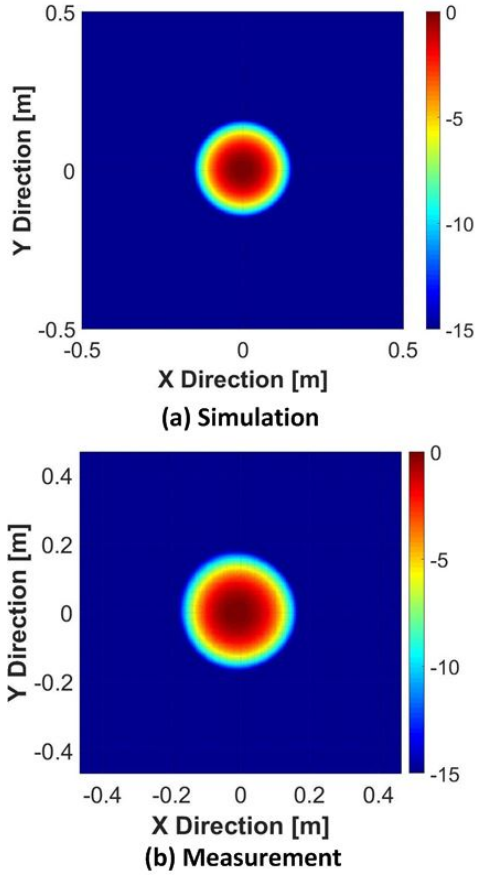

Fig. 5: Focusing pattern for the center focal point

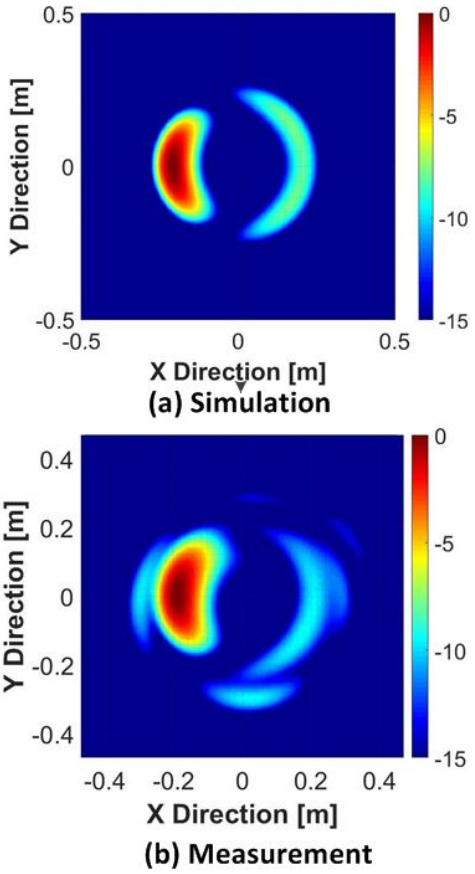

Fig. 6: Focusing pattern for the edge focal point

cularly distributed array elements. Here, it is clear that the form of the sidelobe is almost identical to each other over both azimuths. Its MSLL is about 8 dB for simulation and measurement as seen in Fig. 4 while as seen in Fig. 3 MSLL obtained by measurement is slightly higher than that obtained by simulation. There may be a fact caused by calibration error.

B. Near Field Focusing Pattern

As seen in Fig. 5, the focusing pattern for the center focal point obtained by measurement is compromise by that obtained by simulation. The focusing pattern is circular due to VirtAr-2 distribution and the 15 cm beam-width obtained by measurement is identical to that calculated from simulation data. It is worth noticing that there is no sidelobe in the region of interest.

As the focusing beam is steered to the edge position in Fig 6, it is firstly noticed that the beam-width becomes worse because of the narrower projection of the virtual aperture. Side-lobes for the measurement focusing pattern as seen Fig 6 (b) form by about 8 dB which is identical to that for simulation focusing pattern. Nevertheless, there are some difference on the distribution of side-lobes obtained by simulation and measurement due to the calibration error.

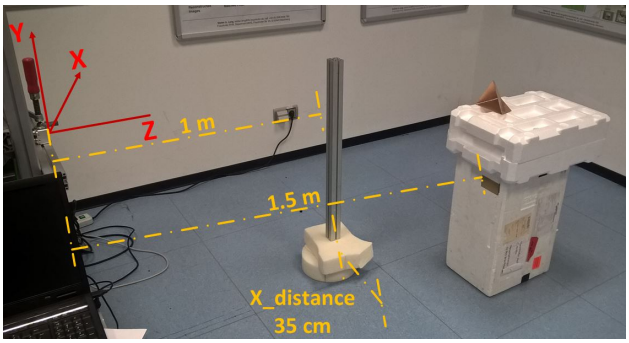

Fig. 7: Positions of Targets

IV. Application within Far Field

The proposed array in Fig. 1 is employed in a real application in order to see its imaging performance. Two metal targets, a metal bar and a corner reflector are positioned at 1 m and 1.5 m range as seen in Fig. 7. The distance between these two targets along the X axis is 35 cm. The measurement is performed at the center frequency of 117 GHz with 12 GHz frequency bandwidth. The MKMA algorithm is used to reconstruct 3D image.

Fig. 8 shows 2D image reconstructed over X and Range axes. It is clear that both targets are well reconstructed in the region of interest at their true positions. It is worth noticing

that the MSLL is also seen nearby metal bar and consistent with the MSLL, about 8 dB presented in the focusing pattern in Fig. 3 and 4.

In Fig. 9, 3D image is presented for 5 dB iso-surface value. It is shown that the image of two metal targets are obtained at their true positions. On the image there is no side-lobe existing due to the iso-surface value which filters them.

V. Conclusion

This paper has proposed a novel MIMO array topology and investigated the focusing patterns and imaging performance of the array.

The proposed array is quite compact with 2 Tx and 8 Rx elements while element sampling is sparse that it brings easiness in terms of manufacturing.

For far field focusing pattern, the obtained cross-range resolution is 8.3^o with 8 dB MSLL. In the region of interest, its dynamic range is not high due to the small number of antenna elements. Thus, this may result in an imaging degradation when strong and weak scatter targets are closely located to each other.

Within the near field, the focusing pattern is circular and does not have side-lobes for the center focal point. When it steers the edge focal point, the beam-width degrades and side-lobes come into view.

In the far field application, the MIMO array is employed to obtain 3D image of two metal targets. The obtained radar image for the targets is well reconstructed and agrees with the far field focusing pattern.

The MIMO array, proposed in this work, is an intermediate step in order to develop a MIMO radar providing high resolution with more Tx and Rx elements, called as high resolution radar camera (HRRC). Next work will mainly focus on the design and development of HRRC.

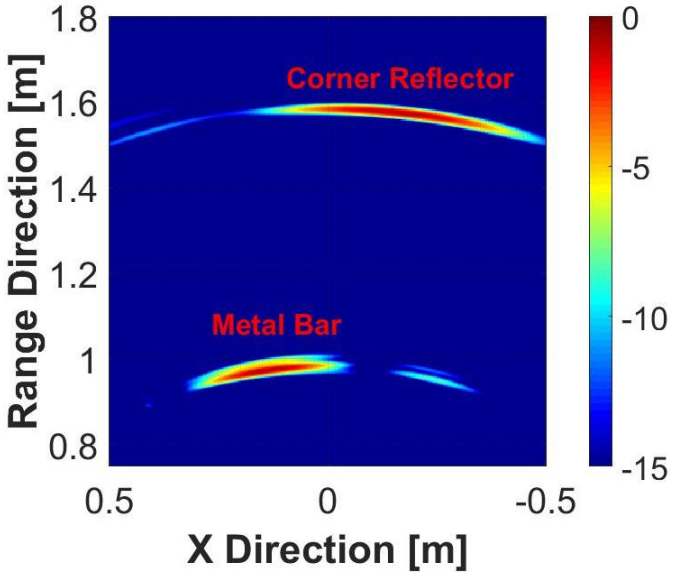

Fig. 8: 2D reconstructed image

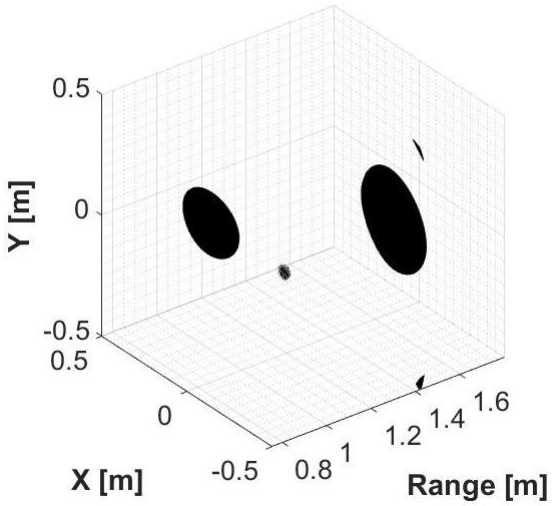

Fig. 9: 3D reconstructed image by 5 dB isosurface val.

Acknowledgment

SmokeBot is funded by the European Commission Seventh Framework Programme for Research, Technological Development and Demonstration under Grant Agreement 645101.

References

[1] R. Appleby, R. N. Anderton, *Millimeter-wave and submillimeter-wave imaging for security and surveilance*, Proc. IEEE, vol. 95, no. 8, pp. 1683-1690, Aug. 2007.

[2] J. H. G. Ender, J. Klare, *System architecture and algorithms for radar imaging by MIMO-SAR*, Radar Conference, 2009, pp. 1-6.

[3] D. M. Sheen, D. L. McMakin, and T. E. Hall, ?Three-dimensional millimeter-wave imaging for concealed weapon detection,? IEEE Trans. Microw. Theory Tech., vol. 49, no. 9, pp. 1581?1592, Sep. 2001.

[4] *http://aass.oru.se/Research/mro/smokebot/*

[5] X. Zhuge and A. G. Yarovoy, *Study of Two-Dimensional Sparse MIMO UWB Arrays for High Resolution Near-Field Imaging*, IEEE Trans. Antenna Propag., vol. 60, no. 9, pp. 4173-4182, Sept. 2012

[6] H. Cetinkaya, S. Kueppers, R. Herschel, N. Pohl, *Comparison of near and far field focusing patterns for two-dimensional sparse MIMO arrays*, Antennas and Propagation (EuCAP), Davos, Switzerland, 2016.

[7] X. Zhuge, A. Yarovoy, *A Transducer Array of an Imaging System*, NL Patent 2008725, Nov. 06, 2013.

[8] L. S. Biller, G. E. Friedman, *Optimization of Radiation Pattern for an Array of concentric Ring Sources*, IEEE Trans. Audio Elec.Acoustics, vol. 21, no.1, pp. 57-61, 1973.

[9] J. W, Sherman, *Properties of Focused Apertures in the Fresnel Region*, IRE Trans. Antenna Propag., vol. 10, iss. 4, pp. 399-408, July 1962.

[10] H. Cetinkaya, S. Kueppers, R. Herschel, N. Pohl, *Comparison of near and far field focusing patterns for two-dimensional sparse MIMO arrays*, Antennas and Propagation (EuCAP), Davos, Switzerland, 2016.